

Automation of Testing of Polymer HVDC Cables using Controlled Rapid Voltage Surges.

Thomas Karlsen

Master of Science in Energy and Environment
Submission date: June 2007
Supervisor: Erling Ildstad, ELKRAFT

Problem Description

Due to and commercialization of the energy markets and environmental considerations there is an increasing interest in large-scale exchange of power between different countries and continents.

For the highest rated voltages in DC today, only oil-impregnated paper is utilized as cable insulation. Extruded polymer solutions are currently being developed but many questions are still unanswered. This is connected to among others, choice of testing methods for documentation of high production quality and good long-term properties. The test procedure chosen must be relevant regarding the service stress and sensitive for detection of production weaknesses.

In a NFR- and industrially supported project it is at NTNU/SINTEF being worked on developing a simplified voltage surge technique for detecting insulation weaknesses in high voltage DC insulation.

It has been shown that initiation of electrical trees in polymeric cable insulation can occur from contaminations when being subjected to abrupt surges at a voltage significantly lower than the breakdown voltage.

With basis in the developed experimental circuit, the student shall develop an automated system that will replace the manual performing of subsequent rapid voltage surges and detecting cable failures.

Assignment given: 15. January 2007
Supervisor: Erling Ildstad, ELKRAFT

Summary

This report aims to describe the work done in order to develop and create a solution for automation of failure detection and performance of rapid voltage surges. The automated system was developed with basis in the experimental circuit developed at NTNU/SINTEF. The circuit relied on manually performing rapid voltage surges and detecting cable failure. Meaning that inequality in the performance of each grounding may introduce unknow variables.

The realized automation system consisted of two parts. The first part was a switch that was able to withstand the voltage applied and able to perform the rapid voltage surges. The second part was a program that controlled the switch and regularly monitored the condition of the cable object, indicating failure when electrical treeing had caused breakdown in the cable insulation.

Two solutions for switches were examined. One switch utilized an arm moving between two electrodes for grounding the objects, using textile bakelite as insulation and support frame for the electrodes. The other switch utilized a sphere gap with air as insulation and an electric field strength close to the breakdown strenght of the air. Groundings in the sphere gap switch were performed using a striker to greatly enhance the electric field and cause a spark between the spheres, causing a transition from a highly insulating state to a highly conductive state.

As the experimental circuit had a large current limiting resistance, the experimental circuit was sensitive to leakage currents as they set up a voltage over the resistance, instead of the cable objects. Leakage currents in the switches were examined and it was found that the arm switch had leakage current unacceptable for use in the experiment. Similarly, leakage currents in the sphere gap switch were examined and found to be acceptable for use in the experiment.

The behaviour of cable objects that, due to electrical treeing had developed insulation failure was examined and measurement parameters for detecting cable failure were found. These parameters were implemented using LabView as a platform for creating a a control program and interface to the instruments connected to the switch.

Having fully created the automated system, the system was used in testing cable objects and was found able to inflict and detect a cable failure due to electrical treeing. However, compared to previous results, a lower number of groundings was needed, which may indicate that the introduction of the sphere gap switch has altered the circuit in a manner such that new results

will differ from former results.

Contents

1	Introduction	1
1.1	Sample and electrode arrangement.	2
1.2	Spark gaps	3
2	Development and testing	4
2.1	General Program control	4
2.1.1	Measuring current	4
2.1.2	Program requirements	6
2.1.3	Program design	8
2.1.4	Testing of the program	14
2.2	Arm switch	15
2.2.1	Design	15
2.3	Sphere gap switch	19
2.3.1	Design and simulation	21
2.3.2	Arrangement	22
2.3.3	Control circuit	22
2.4	Testing	26
2.4.1	Testing of withstand values	26
2.4.2	Testing of leakage currents in the arm switch	27
2.4.3	Testing of leakage currents in the sphere switch	27
2.4.4	Testing of a cable object using the sphere switch	28
3	Results	30
3.1	Program	30
3.2	Arm Switch	31
3.3	Sphere switch	33
3.4	Closer examination of the undetermined leaked current	37
4	Discussion	43
5	Conclusion	45
6	List of devices	46
A	Monitor voltage and output current	48
B	Maximum E-field at electrode surface	48
C	Voltages measured with sphere switch	50

List of Figures

1	Experimental circuit for use in testing.	2
2	Currents measured in a cable with failure	5
3	ABC equivalent for measuring partial discharges	7
4	Shunt for measuring partial discharges	7
5	Flowchart for the control program	9
6	Start loop of the program.	10
7	Labview implementation of equation 18.	10
8	Sequence of closing and opening the breakers.	11
9	Front panel of the program	12
10	Electric field versus radii of electrodes.	16
11	Electric field versus separation distance.	17
12	Contour of electric field for radius and separation distance. . .	17
13	Electric field between electrodes.	18
14	Supportplate for switch electrodes.	19
15	IEEE standard for vertical sphere gap	21
16	Electric potential when needle strikes	22
17	Electric field strength when needle strikes	23
18	Sphere gap arrangement	24
19	Control circuit for needle	24
20	Circuit for measuring current through sphere gap	28
21	Monitor voltage versus output current	30
22	Currents with and without armbreaker in circuit.	32
23	Calculated voltage loss with armbreaker in circuit.	33
24	Measured withstand values and table values	35
25	Breakdown channel in cable insulation	36
26	Breakdown channel in cable insulation	38
27	Measured current with no equipment connected.	39
28	Inner resistance of source	40
29	Relation between monitor voltage and output current	41

List of Tables

1	Values of disruptive-discharge voltages valid for direct voltages of either polarity. From [6].	20
2	Measured current and deviation from calculated current.	31
3	Monitor voltages without any equipment, and with arm switch in circuit.	32
4	Measured Gap distance and withstand voltage	34
5	Measured voltages from control circuit	35
6	Voltages measured with shortcircuited gap and the currents they indicate	37
7	Deviation of measured currents from calculated current	37
8	Calculated current and resistance in voltage divider	41
9	Calculated currents through R1	42
10	List of devices	46
11	Measured monitor voltage and calculated current.	48
12	distance = 0.075 m	48
13	distance = 0.1 m	48
14	distance = 0.125 m	49
15	distance = 0.15 m	49
16	distance = 0.175 m	49
17	distance = 0.2 m	49
18	distance = 0.225 m	49
19	distance = 0.25 m	50
20	Voltages measured with 3.69 cm gap distance	50
21	Voltages measured with 4.97 cm gap distance	51
22	Voltages measured with 7.10 cm gap distance	51
23	Voltages measured with shortcircuited gap.	52

1 Introduction

HVDC transmission has been in use for more than 50 years and has proved to be a reliable and valuable transmission media for electrical energy and has a number of technical advantages compared with HVAC transmission [2]. Improvements in material technology and extrusion methods have made it possible to use polymeric insulation for both AC and DC power cables.

Currently, accumulation of space charge limits the use of polymeric insulated HVDC cables to transmission systems that do not undergo polarity reversals and have a limited voltage range. It is a common perception that one particle or irregularity in the insulation may be sufficient to cause breakdown. This means that it is essential to be able to reveal such weaknesses before installation.

The use of polymeric cable insulation for HVDC cables is highly desirable from a commercial perspective and there is an incentive for use of polymeric insulation even for cables with the highest transmission capacity, today the voltage level of HVDC cables is limited to 600 kV. And so there is a need for further research to gain a more complete understanding of processes involved in space charge accumulation.

A method of testing for such weaknesses has been proposed by Mildrid Seljord and Erling Ildstad [7]. Testing of Rugowski objects with embedded defects had shown that electrical treeing and breakdown can occur at an embedded defect as a result of rapid grounding after DC prestressing at a voltage much lower than the short-term breakdown voltage.

Based on this, the method for testing lengths of cable for weaknesses has been proposed [4]. The method consists of inserting needles into the insulation of cable objects with XLPE insulation and poling the objects in order to provoke space charge injections around the needle tip. The cable objects were then subjected to subsequent rapid voltage groundings. It was found that electrical treeing and breakdown can occur as a result of abrupt grounding after DC pre-stressing at a voltage much lower than the breakdown voltage of the cable. The faster the grounding was done, the more marked was this effect.

When repeated on several test lengths, the procedure should give information about allowable working stress of a cable. If the test procedure would turn out to be successful, it may also be used as a routine test on long lengths of DC cables. However, this method involved that the surges are being performed manually introducing several variables as the surges never will be performed identically each time. The purpose of the work presented is to create and

test an automated method of executing the experiments using controlled rapid voltages surges, by developing and creating a control program and a high voltage switch.

1.1 Sample and electrode arrangement.

The proposed experimental method is described in [4]. Test objects are made using using 1 m long sections of a 12 kV XLPE cable equipped with terminations. In each test object, a sewing needle, with a tip radius of 50 μm , and an overall diameter of 0.8 mm was at room temperature inserted through the insulation screen and into the XLPE insulation. A mechanical tool was specially designed to make reproducibly selected distances between the needle tip and the conductor screen. In addition, a metallic mesh was clamped to the insulation screen to fascilitate high frequency grounding of the screen and needle.

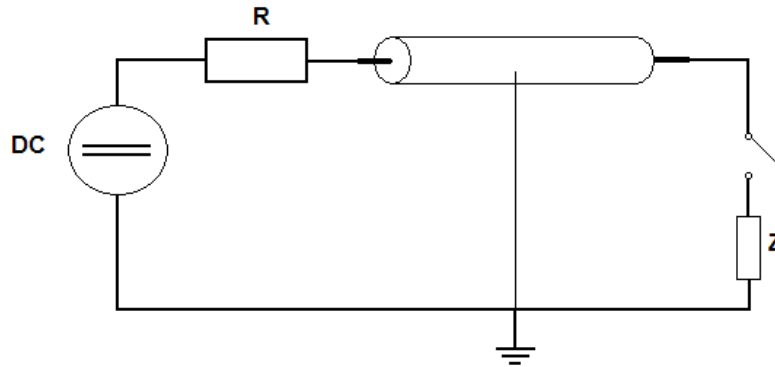


Figure 1: Experimental circuit for use in testing.

Before grounding the cable objects, the applied voltage was increased to the prestress level and held at this level for 24 hours. When closing the grounding switch, the voltage was rapidly reduced to zero at a rate determined by the capacitance of the test object and the impedance Z , of the grounding circuit. The high voltage resistance of $R = 2.005 \text{ G}\Omega$ made it possible to operate this switch independent of the DC source and reduced the short-circuit currents from the source.

1.2 Spark gaps

Simple spark gaps insulated by atmospheric air can be used to measure the amplitude of a voltage above about 10 kV. As the fast transitions from an either completely insulating or still highly insulating state of a gap to the high conducting arc state is used to determine a voltage level, the disruptive discharges does not offer a direct reading of the voltage across the gap. A complete short-circuit is the result of a spark, and therefore the voltage source must be capable to allow such a short-circuit, although the currents may and sometimes must be limited by resistors in series with the gap.

Osmokrovic et al [10] used a three-electrode spark gap to create a method of testing high-voltage circuit breakers with rated power values up to 25000 MVA under short-circuit conditions. As the maximum short-circuit power obtainable from an actual grid was 6000 MVA, they increased the power by building a synthetic circuit together with a direct test circuit. These were synchronized using a three-electrode spark gap.

Two different types of three-electrode gas insulated spark gaps were used; a spark gap with a third electrode beeing inside the main low-voltage electrode. And a spark gap with a separate third electrode on floating potential. The spark gap triggering was realized by applying a negative triggering pulse to the triggering electrode, setting up a greater voltage difference than the DC breakdown voltage and initiating a breakdown.

2 Development and testing

2.1 General Program control

Labview software was used to control and monitor the applying of rapid voltage surges. The name is short for Laboratory Virtual Instrumentation Engineering Workbench and is widely used for data acquisition, instrument control, and industrial automation. It also features a platform for a visual dataflow programming language similar to Matlab's simulink.

The instrument chosen for controlling the test was a HP Agilent 34970A data acquisition/switch unit. The instrument can communicate with a computer using either a GPIB- or RS-232 interface [1]. In addition the instrument is extensible with up to three plugin-modules. The two modules that were chosen was a 20 channel armature multiplexer and a 4x8 two-wire matrix switch. This enabled the control system to both measure voltages from up to 20 inputs and perform any possible connection at 32 crosspoints in the matrix switch¹.

2.1.1 Measuring current

As surges are applied, an electrical tree will form from contaminations in the cable insulation. Such contaminations will enhance the electric field, causing partial discharges and a failure will occur. When this failure occurs, a conductive breakdown channel will appear and a significantly larger current will flow through the circuit.

In order to detect these failures, a specific voltage given from the glassman HV-source was used, the *monitor voltage*. The user manual [5], claims that this monitor voltage is a 0 - 10 V signal in direct proportion to output current from the source.

For determining the actual relation between monitor voltage and the output current of the source, a circuit consisting of only two resistances was set up. These resistances was the same as the current limiting resistances for testing cable objects and had a value of 2 G Ω plus 5 M Ω . The applied voltage was read from the display at the front panel of the source and the monitor voltage was measured with the Agilent unit.

¹As the power needed to operate the circuit breakers will exceed the rated switching values of the instrument, the matrix switch will route a 12 V signal to relays capable of switching this power.

For some of the applied voltages, the voltage over the resistance of $472.6 \text{ k}\Omega$ was measured, and the belonging current was found. Also, the deviation from the calculated current in table 11 was found. See table 2.

The total resistance would then be $2.005472600 \text{ G}\Omega$, and the calculated current was found simply using ohms law:

$$\text{calculated current [A]} = \frac{\text{Applied voltage [V]}}{2.0054726 \cdot 10^9 \Omega} \quad (1)$$

The applied voltage, the measured monitor voltage and the calculated current can be seen in table 11 in appendix A.

A relation between the monitor voltage and the current in the circuit was derived. As seen in figure 21, the approximation is fairly accurate. And this relation was further used in the labview software as a method of determining the output current from the source.

A cable with a known failure was inserted into the circuit and tested. The resistance of the faulty cable was very low compared to the total resistance. Following, the current through the cable was very similar to the current measured when the circuit consisted only of the resistances. In figure 2 the current through a faulty cable is plotted together with the current measured when short-circuiting the cable object.

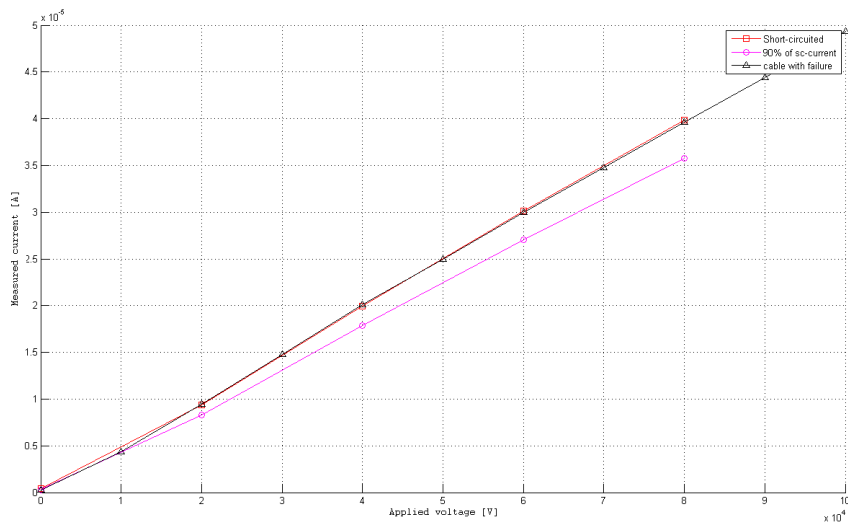


Figure 2: Currents measured in a cable with failure

As seen in figure 2, a cable with a failure in the circuit, represented a connection from conductor to shield with no significant increase in the total resistance, about 50 M Ω [11]. This meant that no significant decrease from the short circuit current. When introducing a interval from the maximum current, this was used as a parameter for detecting a cable failure.

2.1.2 Program requirements

Testing of a cable object consists of poling a cable object with needle implants for 24 hours so that the slow polarisation mechanisms have decayed. When this is done, the cable object is subjected to repeated negative rapid voltage surges by bringing the conductor voltage to ground. This is done with a fixed time interval. This performing of rapid voltage surges takes place until the cable object grow electrical trees and an electrical breakdown occurs.

It is the intention that when the cable breaks down, the failure shall be detected by the program and the number of groundings displayed. Each measurement as well as the number of grounding were to be displayed on a graph and later stored in a datafile.

As the current that flows through the point of failure will vary, it is desired that the failure indicating interval is adjustable from the user panel of the program.

Additionally it is desired to measure any partial discharges that may occur in the initial growth of the electrical tree. This measurement would done by using the abc-equivalent of an initial electrical tree, see figure 3.

A rough calculation of the needed sensitivity can be done when using the equation for stored energy in a capacitor $Q = C \cdot U$ and assuming the capacitance cable of the cable as 200 pF and the dissipated charge in a partial discharge as 1 pC. The measurement equipment will be performed in another project but as the same control software will be used, the implementation was done here/now.

$$U = \frac{Q}{C} = \frac{1 \cdot 10^{-12} C}{200 \cdot 10^{-12} F} = \frac{1}{200} V = 5 \text{ mV} \quad (2)$$

As the equipment for measuring these partial discharges needs to be very sensitive, the shunt needs to be protected during the relatively violent voltage surge. This was done by inserting a breaker B1, that protects the shunt by connecting it to ground it as shown in figure 4, and creating a alternate path

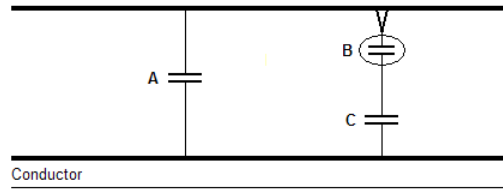


Figure 3: ABC equivalent for measuring partial discharges

for the current. The required action of the program is to close this breaker before the surge and then open it after the surge.

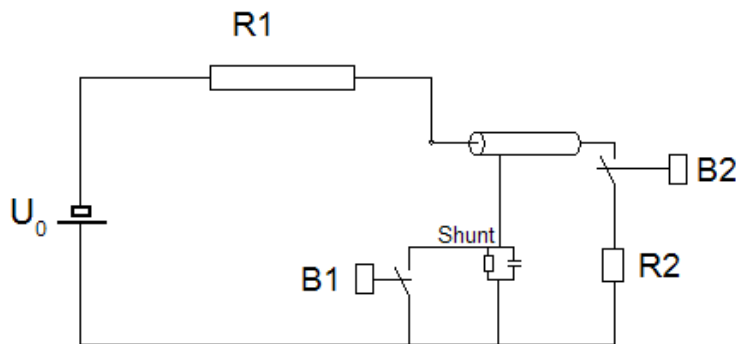


Figure 4: Shunt for measuring partial discharges

All these requirements for the program and control circuit was summarized into the follows:

- Perform the desired number of voltage surges until failure.
- The voltage surges shall be performed with a fixed intervall.
- Regularly check for failure between the surges.
- Protect the equipment measuring partial discharges.
- Display the measurements.
- Save the measured data to a file.

2.1.3 Programdesign

In order to better structure the requirements and behaviour of the control program, a flowchart was needed in order to perform the design. A flowchart is a schematic representation of the process, and helps creating the program code. This is especially useful when programming in labview, which is a visual programming language. When applying the requirements listed earlier, a flowchart was drawn as in figure 5.

The flowchart summed up the main tasks to be performed by the program. However, due to the nature of the programming language in labview, the program itself needed to be more complex.

From the flowchart, the program was divided into three sections. The first section took care of the "start test" part in the flowchart. In this section, all the necessary input parameters are collected before continuing. The realization of this was to use a while-loop that runs continuously until a start-button is pressed. This loop collects the parameters and initiates the main part of the program when the button "Start test" is pressed, see figure 6.

It would be convenient only to enter the applied voltage as a parameter for determining the maximum current. But as the current limiting resistances can be replaced, this is entered in addition to the applied voltage. Further the relation in equation 18 was implemented for finding the belonging monitor voltage, see figure 7.

When the start-button is pressed, the parameters are collected and a VISA² connection to the instrument is created. When this is done, the program exits the initial loop and the second part of the program is started.

The second and main section of the program took care of the two loops that can be seen in the flowchart, figure 5. In this section, groundings and failure-checks are performed. Groundings are performed by routing a 12 V signal to a relay, using the 4x8 matrix switch.

The realization of the second section, and main part of the program, was done using two nested loops. The outermost is a for-loop that is governed by the execution of surges and runs for the number of times set in "number of surges" at the start of the program. The innermost is a while-loop that is governed by the measurements performed between the surges.

When in the while-loop, the program will measure the monitorvoltage using the 20-channel multiplexer and use this to check for cable failure. This will

²Virtual Instrument Software Architecture

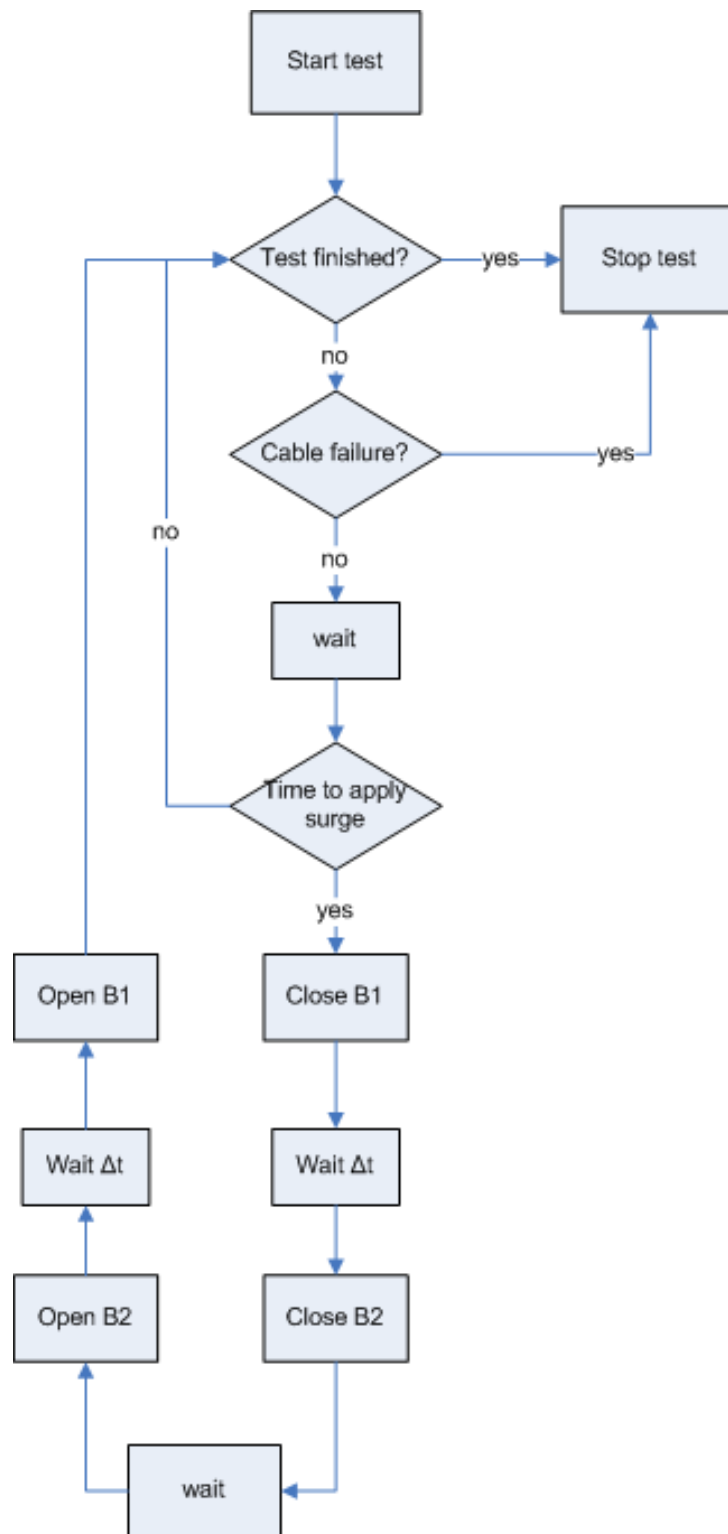


Figure 5: Flowchart for the control program

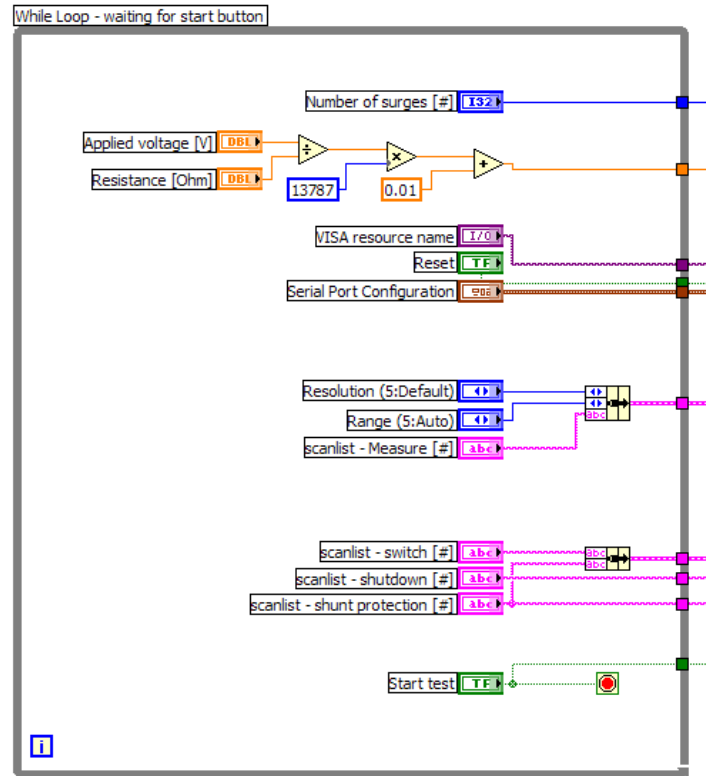


Figure 6: Start loop of the program.

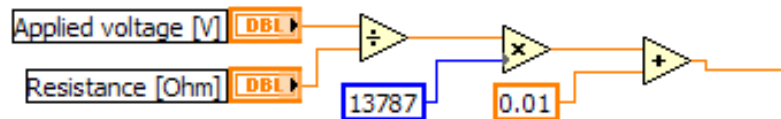


Figure 7: Labview implementation of equation 18.

be done with a fixed interval until it is time to perform the next grounding. The time between each measurement is set from "measure interval" at the front panel of the program. The currents indicated by the measured monitor voltage is displayed as a graph in the right section of the frontpanel. If a failure is detected, the program will close the breaker protecting the pd-shunt, open the latch, show a message dialog and stop.

When the surge interval has elapsed and no failure has been detected, the program exits the inner while loop and performs a grounding. The performance of a grounding is realized with a sequence of closing and opening the two relays, B1 and B2, see flowchart 5. At first, the relay that protects the pd-shunt, B1, is closed. Then the program waits a time "shunt w-time" before closing the relay B2, that performs the actual grounding. When the program then has waited the "coil discharge time", it opens the relay B2, and again waits the time "shunt w-time" before opening the relay B1. See figure 8 for the realization of the sequence in labview.

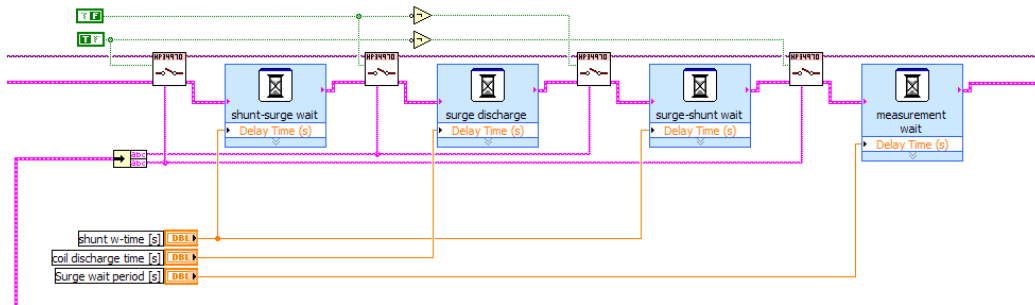


Figure 8: Sequence of closing and opening the breakers.

When grounding has been performed, the for loop either continues or exits. This is dependent on whether the desired number of groundings has been reached or not. If not, the for-loop continues. And if the desired number of groundings has been performed, the program closes the breaker that is protecting the pd-shunt, opens the latch and stops.

When the Labview code of the program was fully created, a front panel was designed. The front panel is the graphical user interface used when running the program and synthesises the behaviour of a real instrument. For this reason it is also called a virtual instrument, [8].

Mainly, the front panel consists of datafields for entering the parameters that are required in the initial while-loop, see figure 6. It also includes an

area that shows the progress of the test and an area that displays the latest measurements of output current. See figure 9 for the design of the front panel.

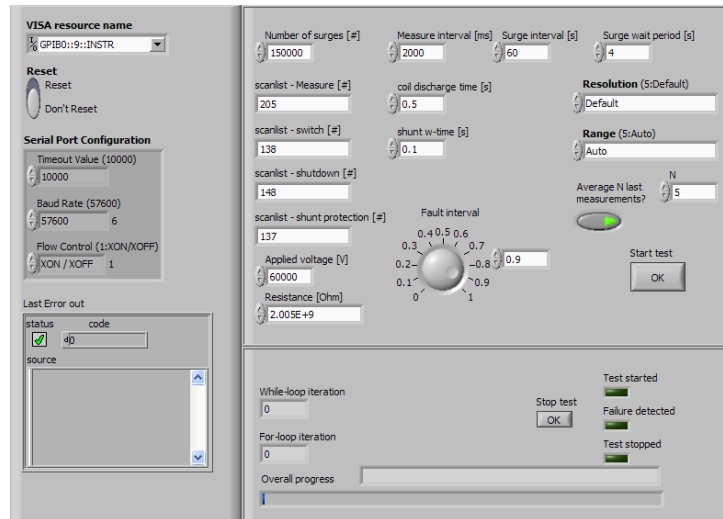


Figure 9: Front panel of the program

The program controls four channels on the Agilent instrument. One for measuring the monitor voltage, the second for triggering the switch and the fourth for protecting the equipment for measuring partial discharges. The third is optional and can be used for latching of the HV-source when the program has detected a failure in order to stop the current flowing through the cable insulation.

All the datafields in figure 9 is explained as follows:

VISA resource name This is the field for specifying the GPIB-adress for the instrument. This value must be the same as the value set at the instrument as there can be several instruments connected to the same cable. Default GPIB channel is set to 9.

Reset This is an option whether to reset the instrument when connecting to it. Default is "Don't reset". Note that this may cause problems if the latch is connected.

Serial Port Configuration This is the configuration when using a RS232 connection instead of a GPIB connection. Default values are set.

Last error out This is a message box that displays the last error message generated. By default, no errors have occurred and the box is empty.

In case a error has occurred, the program should be restarted in order to clear errors and measurement data.

Number of surges This is the desired number of surges that is to be performed. Default is set to a high number, 150000 surges.

Measure interval This is the interval between each check for failure. Default is set to 2000 ms

Surge interval This is the interval between each voltage surge. Default is set to 60 s

Surge wait period When the cable has been subjected to a grounding, a higher current will flow in order for the cable to recharge. Measuring the current in this period may falsely indicate a failure. The wait period is the time the program waits until beginning to check for failure again. Default is set to 4 s

Coil discharge time This is the on-time of the switch, depending on its type type. Default is set to 0.5 s

Shunt w-time This is the time before the surge, that the shunt for measuring partial discharges is protected. This equals the Δt in figure 5. Default is set to 0.1 s

Scanlist - measure The scanlist, indicating where the monitorvoltage is connected. Default is set to channel 205.

Scanlist switch This is the scanlist, indicating where the 12 V is routed to the switch. Default is set to channel 138.

Scanlist shutdown This is the scanlist, indicating where the latch of the HV-source should be connected. This is optional and default is set to channel 148.

Scanlist shuntprotection This is the scanlist, indicating where the breaker for protecting the pd-equipment is connected. Default is set to channel 137.

Applied voltage [V] This is the applied voltage to the circuit and is used for determining the maximum current. Default value is set to 60 kV

Resistance [Ohm] This is the total value of the current-limiting resistances and is used for determining the maximum current. Default value is set to 2.005 G Ω

Fault interval This is the interval used for detecting a failure. When a monitor voltage larger than the product of fault interval and the predicted monitor voltage is measured, the program states that a failure has occurred. Default is set to 0.9.

Resolution This is the instrument resolution for voltage measurements. Default is set to the default setting of the instrument.

Range This is the instrument range for voltage measurements. Default is set to Auto.

N - averaging To avoid being misled by misreadings, one can average over the last measurements in order to better determine a failure. When averaging is used, the average value has to be larger than the product of the fault interval and the predicted monitor voltage. By default, the five last measurements are averaged.

While-loop iteration This is the counter for the while loop and displays the current iteration.

For-loop iteration This is the counter for the for-loop and displays the current iteration.

Overall progress This is a progress bar that displays the progress of the test.

Stop test This is a button that stops the test. It is recommended to use this in order to perform the exiting routines.

Test started This is an indicator that shows whether the test has started.

Failure detected This is an indicator that shows whether a failure has been detected.

Test stopped This is an indicator that show whether the test has stopped.

Plot area This is a graph that displays the measurements of the monitor voltage. The same values are saved to the xml-file.

2.1.4 Testing of the program

During the design process, the program was continuously tested by using a imitated value instead of the real measurement of the monitor voltage. When the program itself worked according to the specitications, the communication with the instrument was tested.

In order to test the voltage measured from the Agilent instrument, a variable low voltage source that could deliver up to 30 V was used to imitate the monitor voltage. The part of the program that checked for failure was finally tested against the glassman voltage source and a cable with a failure.

2.2 Arm switch

A previously used circuit breaker was found to have leakage currents when applying higher voltages. These leakage currents set up a significant voltage over the current limiting resistances. As the applied voltage over the switch increased, the leakage current and hence the voltage over the resistances increased. The voltage over the cable object never reached more than about 40 kV, see [11]

In order to remove this effect of voltage loss, the arm switch was to be modified into a switch with lesser leakage currents.

2.2.1 Design

The initial design was performed with FEMLAB/MATLAB software.

The original switch consisted of a fibreglass plate that held the two electrodes in place. An arm was moved between the electrodes using an actuating coil. The electrodes themselves had a radius of about 0.5 cm. This caused a divergent electric field and a region with high electric stress at the surface of the electrodes.

In order to achieve lesser leakage currents, three main goals were defined for the new design.

- larger radii of the electrodes and edges of the conductive materials.
- larger separation of electrodes in air.
- larger creep distance in the plate between electrodes.

To obtain an initial, but absolutely not final value of the distance between the electrodes for use in the simulation software, the breakdown strength of air was set to $3.2 \cdot 10^6$ V/m. This gives the distance:

$$d = \frac{U}{E_{max}} = \frac{200 \cdot 10^3 V}{3.2 \cdot 10^6 V/m} = 0.0625m \quad (3)$$

A model of two round electrodes were modeled in Femlab. The electrodes were aligned vertically and for fixed separation distances S , between 0.075 m to 0.3 m, the radius was varied from 0.01 m to 0.05 m and the maximum electric field was noted down. The electric field strength was typically highest at the surface of the high voltage electrode. The values are shown in tables 12 - 19 in appendix B.

The results from the simulation were plotted and visualized in matlab. In figure 10 one sees that for all radii, the maximum electric field decreases less as the separation distance between the electrodes increases.

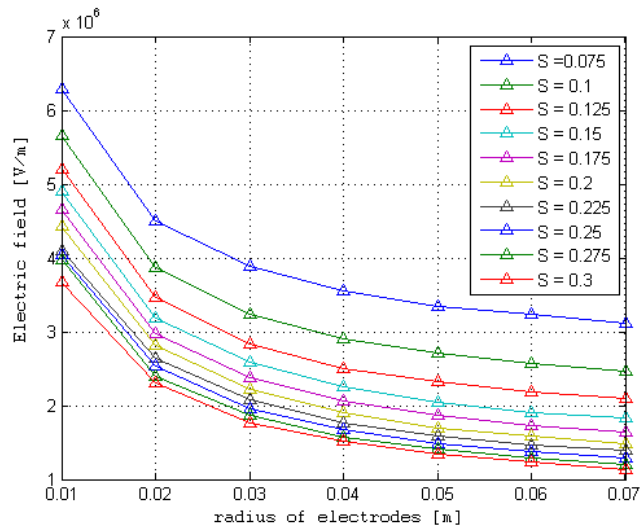


Figure 10: Electric field versus radii of electrodes.

Similar behaviour is seen for the radius of the electrodes, see figure 11. For all separation distances, the maximum electric field decreases less as the radii of the electrodes increases. A good choice of radius and separation distance would be in the area where the maximum electric field is satisfactory low and the dimensions are kept sensibly low.

For better visualisation of the resulting electric field for different values of radius and distance, a contour-plot was plotted for values between 16 kV/cm and 36 kV/cm, see figure 12.

An electrode radius of 0.03 m, and a electrode distance of 0.2 m was chosen based on the availability in the workshop. From the simulation, this gives a maximum electric field of 22 kV/cm at the surface of the HV side of the switch. This configuration is also plotted in figure 12. The actual electric

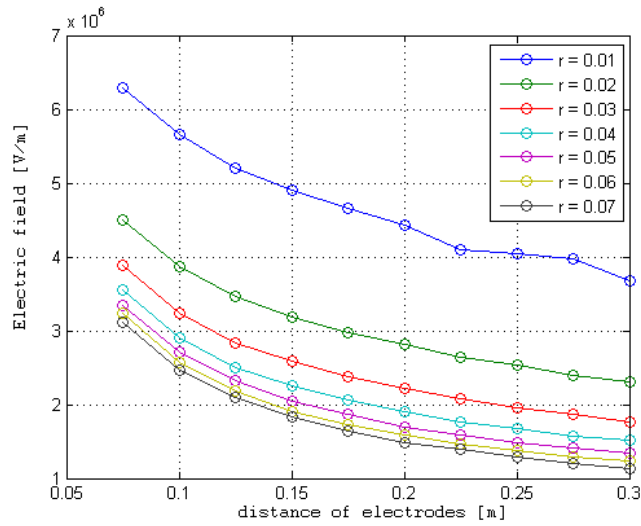


Figure 11: Electric field versus separation distance.

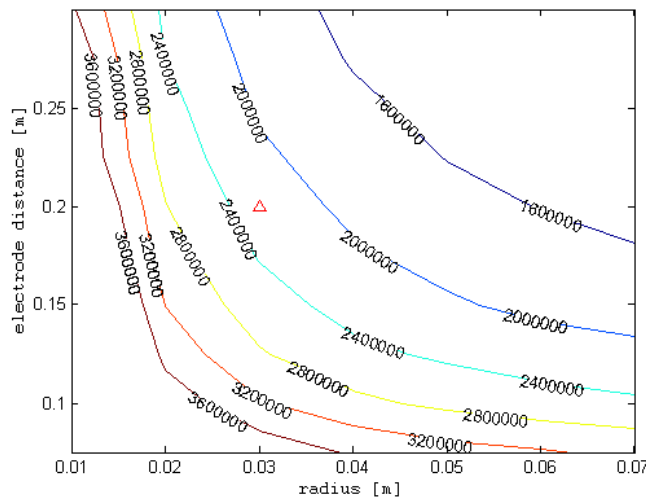


Figure 12: Contour of electric field for radius and separation distance.

field strength along the axis between the centers of the two electrodes can be seen in figure 13. The maximum field strength appears at the surface of the top electrode and is significantly less at the lower electrode. This gives greater tolerances for edges at the arm when the switch is open.

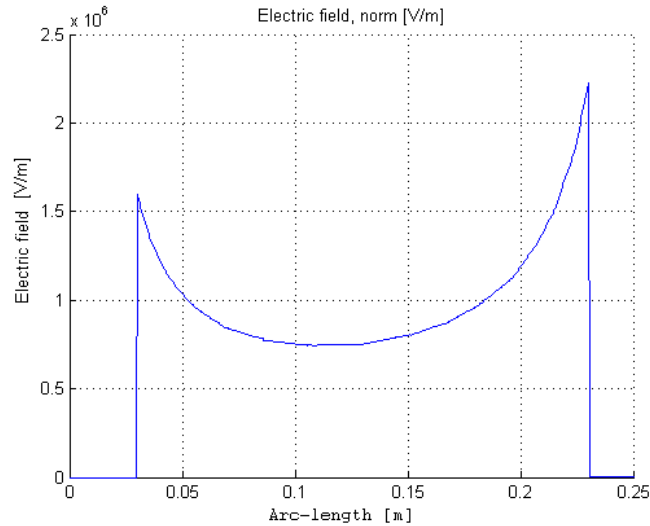


Figure 13: Electric field between electrodes.

A supportplate for the electrodes was designed as in figure 14. The available material for the plate was textile bakelite. This material is often used as insulation for high voltage equipment, as it can endure temperatures up to 120 °C.

The only obtainable material specification from the supplier was that the electrical breakdown strength is 5 kV for 3 mm. The conductivity of the material was unknown.

In the model, see figure 14, the shortest distance between the high-voltage and the ground electrode is about 16 cm. The withstand voltage the plate should then be

$$U_{bakelite} = \frac{5kV}{3mm} \cdot 160mm = 266kV \quad (4)$$

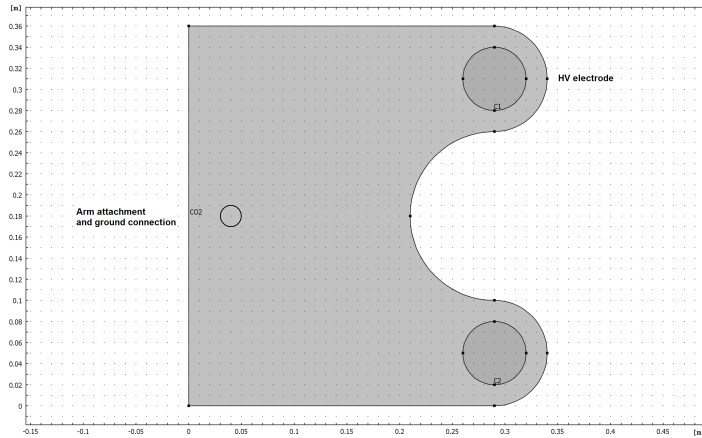


Figure 14: Supportplate for switch electrodes.

2.3 Sphere gap switch

As the arm switch had several divergent fields that were hard to control, a solution with a more homogenous field distribution was needed. Kuffel et al [3] discusses several arrangements for reliably measuring high voltages. Mainly the rod/rod gap and the sphere gap are recommended as their reliabilities are best confirmed.

Rod gaps have earlier been used for for the measurement of impulse voltages, but because of the large scatter of the disruptive discharge voltage and the uncertainties of the strong influence of the humidity, they are no longer allowed to be used as standard measuring devices.

A sphere gap was therefore preferred, as limitation in the gap distance provides a homogenous field distribution between the spheres so that no pre-discharge or corona appears before breakdown. The measuring capability of the sphere gap was not to be used, but the ability to apply maximum voltage before breakdown.

Two methods of modifying a sphere gap into a three-electrode spark gap has been described by Osmokrovic et al [9], but required a relatively complex arrangement. A simpler mechanism of extending the trigger electrode into the sphere gap, would provide similar effect, as the electric field is rapidly increased above withstand level.

A complete short-circuit is the result of a spark. The experimental circuit

has a current-limiting resistance and the voltage source is therefore capable to allow such spark. This would be a good method for performing rapid voltage surges to the cable objects.

The IEEE standard for High-Voltage Testing, [6], defines the standard sphere gap as a peak-voltage measuring device constructed and arranged in accordance with the standards specifications. It consists of two metal spheres of the same diameter, D , with their shanks, operating gear, insulating supports, supporting frame, and leads for connections to the point at which the voltage is to be measured.

Standard values of sphere diameter, D , vary from 62.5 mm to 2000 mm. The spacing between the spheres is designated as S , and varies from 5 mm to 2000 mm. The voltages to be measured with these configurations vary from 69.5 kV to 2490 kV, see table 8 in [6]

Spheres with a diameter of 250 mm were available at the Elkraft engineering workshop. The Glassman HV source provides a dc voltage of up to 200 kV. For the given sphere diameter within this voltage range, the gap distances varies from 25 mm to 80 mm, see table 1.

Table 1: Values of disruptive-discharge voltages valid for direct voltages of either polarity. From [6].

<i>Sphere gap spacing (mm)</i>	<i>Voltage (kV peak)</i>
25	72.5
30	86.0
35	-
40	112
45	-
50	137
55	-
60	161
62.5	-
70	184
80	206

The point on the two spheres that are closest to each other are called sparking points and is where the breakdown occurs. In practice, the disruptive discharge may occur between other neighbouring points. But in the realized switch, a spark will be initiated by rapidly increasing the electric field by moving a striker with a relatively small radius into the electric field between the spheres.

An arrangement, which is typical of sphere gaps with a vertical axis, is shown in figure 15. One sphere shall preferably be connected directly to ground but it may be connected through a resistance for special purposes such as measuring the current when sparks occur. In the interests of personnel and equipment safety, such resistances should be of very low values.

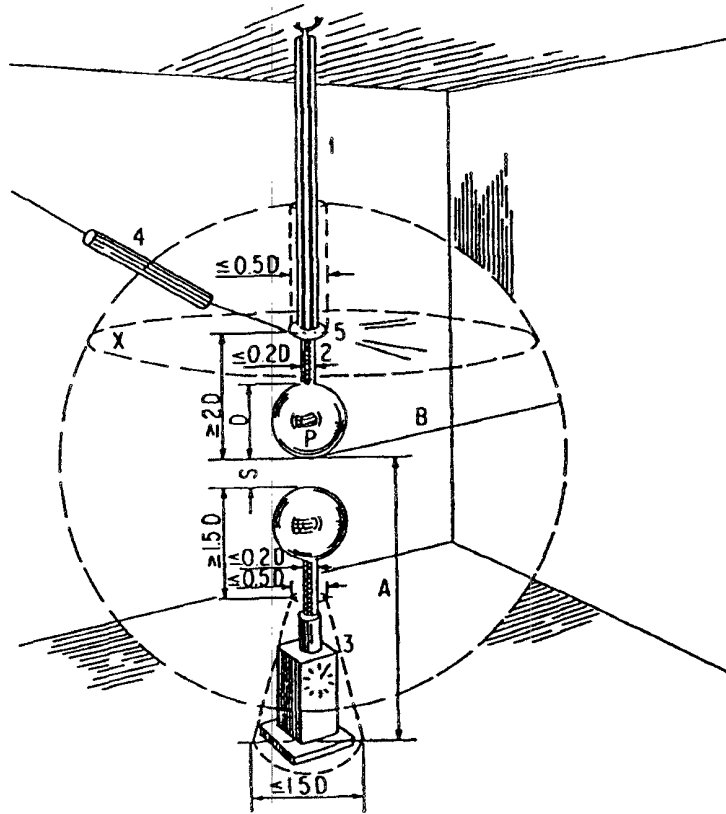


Figure 15: IEEE standard for vertical sphere gap

2.3.1 Design and simulation

The sphere gap arrangement was drawn and simulated with Comsol Femlab software. The model was drawn with the striker pin extended from the lower sphere into the sphere gap. The model was solved and the electric field distribution and the electric potential distribution was found for a case where 86 kV were subjected to a sphere gap distance of 30 mm according to table 1, see figure 16.

It was found that the electric field strength was greatly enhanced at the tip

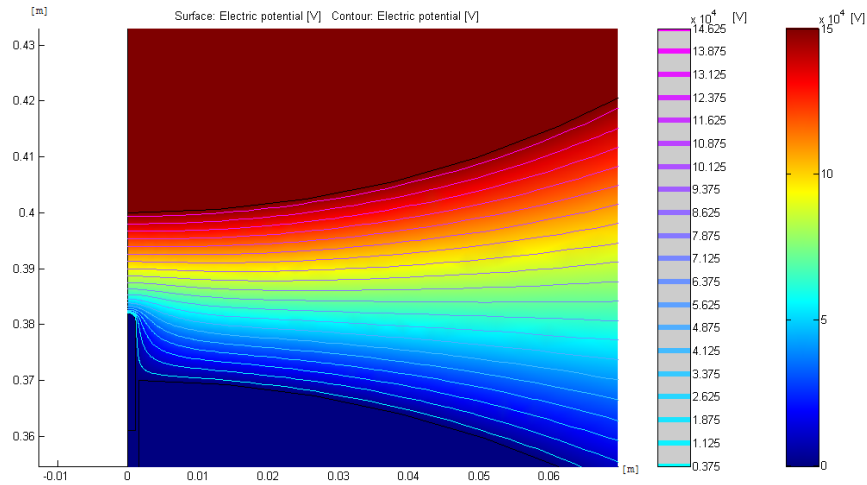


Figure 16: Electric potential when needle strikes

of the striker. A maximum value of the field was found to be as much as 4.6 kV/cm, see figure 17. Finding this, further work with the realization of the switch was performed.

2.3.2 Arrangement

An arrangement consisting of a sphere and a half sphere was set up. The top sphere was connected to the HV side and subjected to the same voltage as the cable objects that were being tested. The bottom half sphere was connected directly to ground. The bottom sphere featured the striker that would be used to rapidly create a divergent electric field, see figure 18. A coil surrounding the striker and would be used to raise the needle into the gap between the spheres.

When the needle is extended into the gap, the electric field around the tip is enhanced above the withstand voltage of the surrounding air. This causes the air to break down and a discharge occurs in the gap between the two spheres.

2.3.3 Control circuit

The lower sphere contained a setup of a striker surrounded by a coil. When a current is led through the coil, the needle is forced up by the magnetic

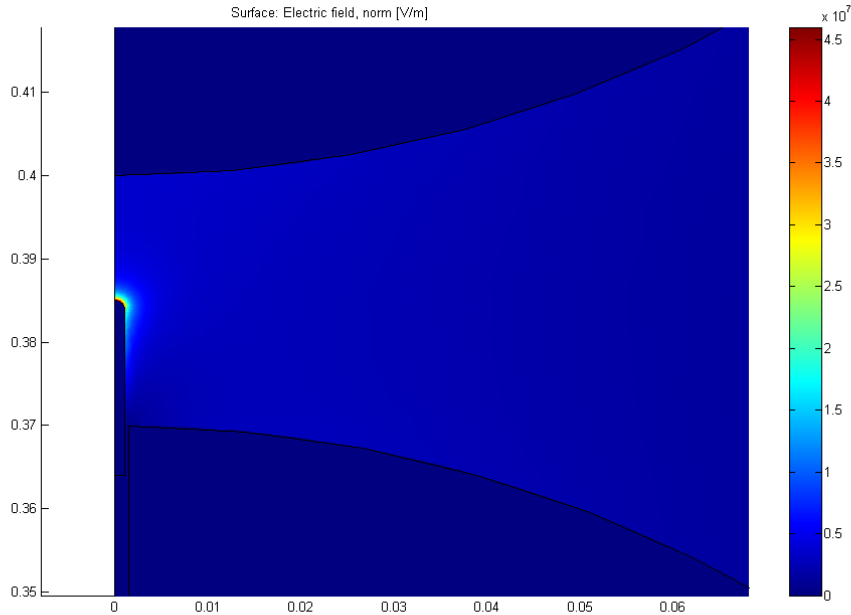


Figure 17: Electric field strength when needle strikes

field. The power needed to actuate the striker was not available from the instrument and therefore a designated electric circuit was created for this purpose, see figure 19.

The Agilent instrument was to control the circuit, routing a 12 V signal to a relay. In order to provide a sufficient amount of energy for the coil to extend the needle, capacitors were to be charged up and discharged over the coil. To charge the capacitors, ac voltage was taken from the grid and transformed down with a 2:1 transformer. Using a fullbridge rectifier the capacitors was charged from both half-waves of the voltage from the transformer.

The energy used when extending the needle would come from the charged capacitors. But in the case of a relay fault, a larger current than intended will flow from the transformer to the coil. Therefore a current limiting resistance R , was inserted in order to prevent the current from exceeding the maximum rated current of the transformer. In addition, fuses were inserted as a general mean of protection.

In order to find a suitable value for the resistance, two relations were to be considered. Firstly, the time constant of the circuit had to be small enough so the capacitors would be fully charged before a grounding were performed.

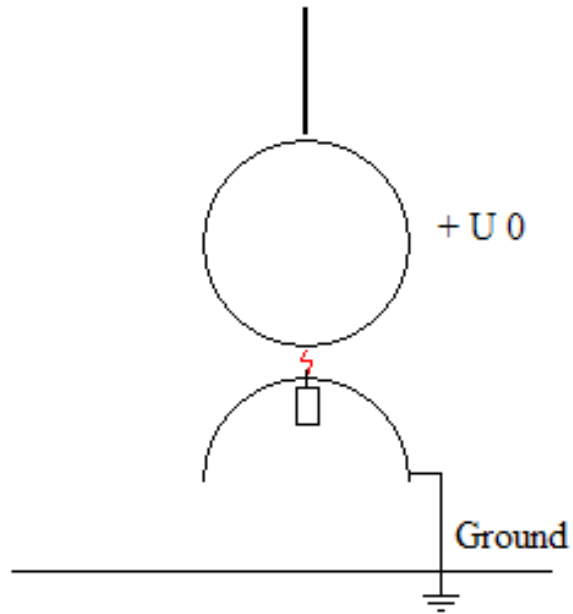


Figure 18: Sphere gap arrangement

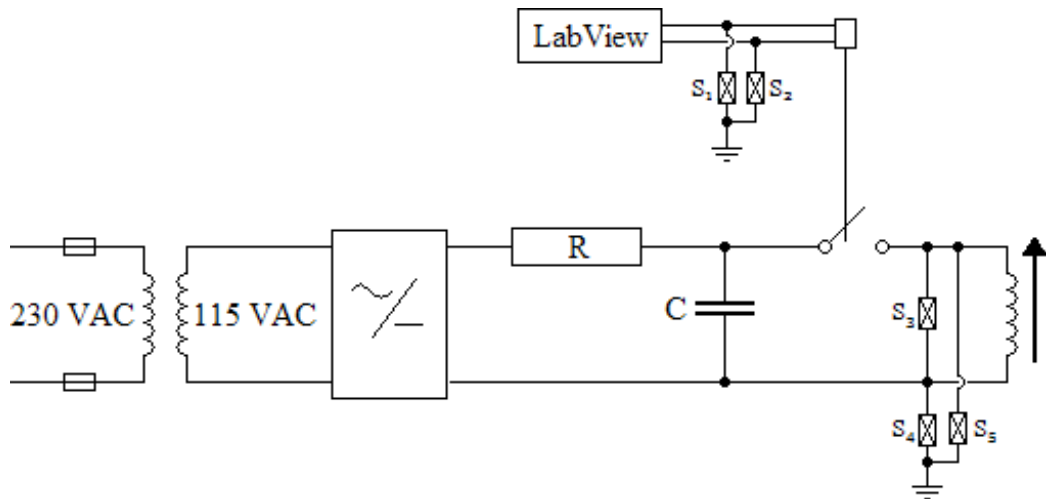


Figure 19: Control circuit for needle

Secondly, the resistance had to be large enough so that the transformer did not deliver more than rated current if the relay was to be closed for a longer period than intended.

The capacitors had to be fully charged within shorter time than the grounding interval of the cable objects, usually 60 s. When the relay is open, the capacitors C , are in series only with the resistance R , and the belonging time constant is $\tau = R \cdot C$. Given that the capacitance is 136 μF , the largest resistance with respect to the first relation is:

$$R = \frac{\tau}{C} = \frac{60s}{136 \cdot 10^{-6} \text{Farad}} = 441176.5\Omega \quad (5)$$

The datasheet for the transformer states that the rated current for the secondary side of the transformer is 250 mA. The rectifier has a rated current of 3 A so the transformer sets the current limit. The rectified voltage over the capacitors was measured to be 177.1 V and the smallest resistance with respect to the second relation was:

$$R = \frac{177.1V}{0.25A} = 708.4\Omega \quad (6)$$

The resistance therefore had to be between 710 Ω and 440 k Ω . A 5 W resistance of 56 k Ω was selected.

In order to protect the circuit itself and connected equipment from incoming overvoltages, five surge arresters were inserted at two places, see figure 19. For protection of the Agilent unit, the two wires connected to the 12 V relay were protected with S1 and S2, having the smallest available protection level of 75 V. The multiplexer can withstand voltages up to 300V and it is therefore assumed able to handle transients up to 75 V.

The output of the circuit was also protected with surge arresters. The protection level of S3, S4 and S5 was set to 225 V, enough to allow the voltage over the charged capacitors to operate the coil surrounding the striker, but also protecting the circuit from incoming overvoltages.

2.4 Testing

2.4.1 Testing of withstand values

A simple test of the withstand values for the sphere gap was performed. According to table 1, the gap distance varies between 2.5 cm and 8.0 cm for the voltages available from the HV source. The sphere gap were adjusted to three different distances within this range, 3.77 cm, 5.02 cm and 7.35 cm. The voltage was then raised until a spark occurred in the gap and noted down, see table 4.

Using the values in [6], the breakdown values corresponding to the distances was found using linear interpolation; for a point (x, y) at a straight line between to points (x_0, y_0) and (x_1, y_1) , the linear relation yields:

$$\frac{y - y_0}{y_1 - y_0} = \frac{x - x_0}{x_1 - x_0} = \alpha \quad (7)$$

For each gap distance, the α from the table was calculated:

$$\alpha_1 = \frac{3.77 - 3.5}{4.0 - 3.5} = 0.54 \quad (8)$$

$$\alpha_2 = \frac{5.02 - 5.0}{5.5 - 5.0} = 0.04 \quad (9)$$

$$\alpha_3 = \frac{7.35 - 7.0}{7.5 - 7.0} = 0.70 \quad (10)$$

Equation 7 was rewritten into:

$$y = y_0 + \alpha(y_1 - y_0) \quad (11)$$

Using these values and equation 11, the corresponding breakdown values was found and is shown in equations 12 - 14.

$$T_1 = 99 + 0.54(112 - 99) = 106.02 \quad (12)$$

$$T_2 = 137 + 0.04(149 - 137) = 137.48 \quad (13)$$

$$T_3 = 184 + 0.70(195 - 184) = 191.7 \quad (14)$$

The percentual deviation of the measured values from the interpolated values was found using equation 15, see alignment 21 - 23.

$$deviation = \frac{U_{measured} - T_{table}}{T_{table}} \cdot 100 \quad (15)$$

2.4.2 Testing of leakage currents in the arm switch

The only known electric property of the textile bakelite used for the arm switch plate, was the breakdown voltage. This was assumed to be a value that is valid for ac voltages only. The dc conductivity was unknown and a testing of any eventual leakage current between the electrodes was performed.

The monitor voltage from the voltage source indicated a current flowing even when no equipment was connected to the high voltage side of the source. As this was a current not accounted by any apparent path, it was believed to be discharges into air. Therefore the currents were measured with and without the breaker in circuit, and the difference between them assigned to leakage in the breaker.

In order to verify the measurements when inserting the breaker, a resistance of 472.6 k Ω was connected between the low voltage electrode and the ground. In order to protect the multimeter in case of discharges, the resistance was protected with a surge arrester with a protection level of 75 V. Voltage over this resistance was measured and the actual current was found using Ohms law.

Voltages from 0 kV to 120 kV was applied and the belonging monitor voltage was measured from the glassman source, see section 3.2.

2.4.3 Testing of leakage currents in the sphere switch

A set of measurements was performed in order to determine the leakage currents through the sphere gap. The multimeter was connected to the lower side of the sphere and protected with a gas arrester in case of discharge. The protection level of the arrester was 75 V. The resistance was inserted into the circuit as R2 in figure 20.

The currents was measured for three gap distances, 3.69 cm, 4.97 cm and 7.10 cm. Three voltages was measured; the voltage applied, the monitor

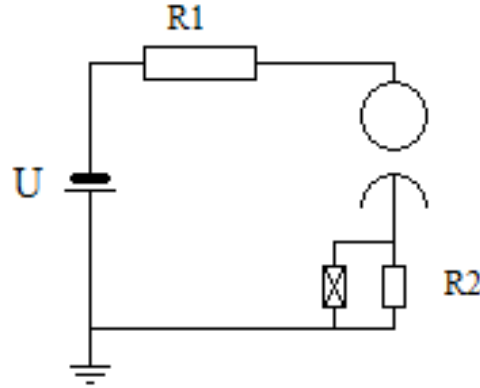


Figure 20: Circuit for measuring current through sphere gap

voltage from the source and the voltage over the resistance R2. As the voltages measured over R2 were too small to be correctly measured by the multimeter, the gap was short-circuited in order to achieve larger currents. These were compared to the monitor voltage in order to verify the currents. See tables 20 - 23 appendix C.

2.4.4 Testing of a cable object using the sphere switch

A cable object was tested using the sphere switch and the program developed in LabView. The applied voltage was 60 kV, the sphere gap distance was set to the lowest in table 1, and the maximum current at failure would then be:

$$I_{max} = \frac{60 \cdot 10^3 V}{2.005 \cdot 10^9 \Omega} = 29.93 \mu A \quad (16)$$

The belonging monitor voltage, the failure parameter, was found applying the relation in equation 18:

$$U_m = 13787 \cdot 29.92 \mu A + 0.01 = 0.4226 V \quad (17)$$

This value was used as the monitor voltage indicating failure and entered into the program. The rest of the default values was not altered.

A needle was inserted into the insulation of the cable object. The cable object was then connected to the sphere switch in series with a resistance of 93.3Ω . This resistance was placed in the circuit in order to control the front time of the grounding pulse.

After poling, the cable object was subjected to rapid voltage surges using the sphere switch and the program created in labview.

3 Results

3.1 Program

The measured monitor voltage was plotted against the calculated current in the circuit using Matlab, see figure 21. The regression tool in Matlab yielded a linear relation between monitor voltage and output current found in equation 18.

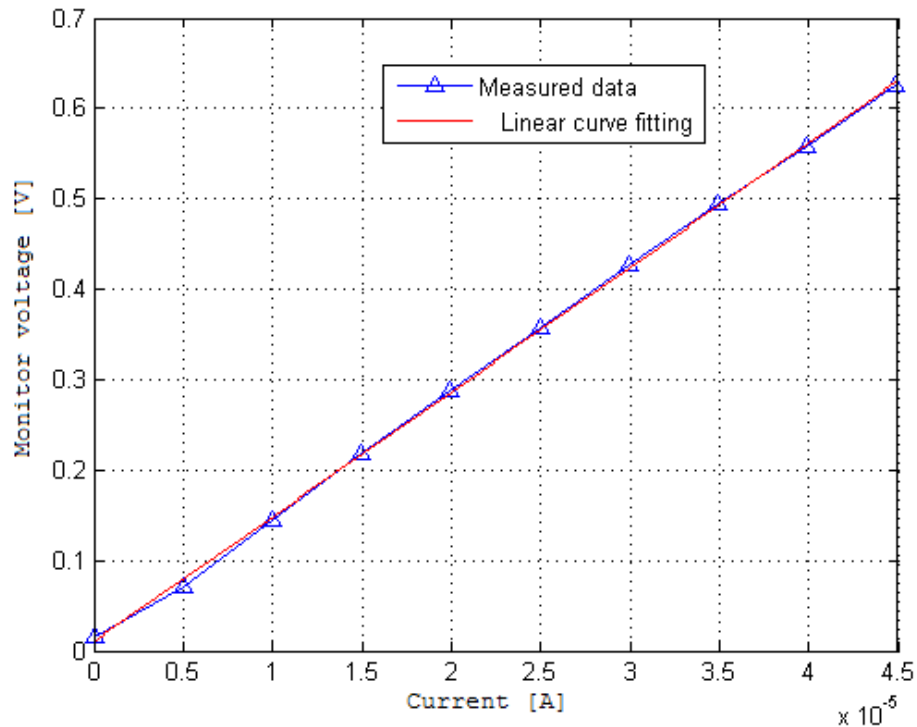


Figure 21: Monitor voltage versus output current

$$U_m(I) = 13787 \cdot I + 0.01[\text{V}] \quad (18)$$

For some of the applied voltages, the voltage over the resistance of 472.6 k Ω was measured, and the belonging current was found. Also, the deviation from the calculated current in table 11 was found, see table 2.

The deviation was found to be small, no more than 1.8 %. When implementing the measurement of monitor voltage and using a interval from maximum

Table 2: Measured current and deviation from calculated current.

U [kV]	Measured Voltage [V]	Measured current [microA]	Deviation
0	0.001	0.002	-
20	4.79	10.14	1.6 %
40	9.38	19.85	0.5 %
60	14.15	29.94	0.1 %
70	16.20	34.28	1.8 %

current in circuit, the program correctly detected a failure.

3.2 Arm Switch

In order to improve a previously used armswitch, a new design was created and tested. Using Comsol/Femlab software, the electric field distribution around two electrodes was plotted for a set of different sizes and distances of the actual electrodes. In all cases the highest values appeared at the surface of the top HV electrode facing the lower electrode.

A configuration of electrode radius equal to 0.03 cm and an electrode separation equal to 0.2 m was chosen, based on the availability in the workshop and the mapping of results from the simulations.

Apart from the breakdown strength, electrical properties for the material used making the armbreaker plate were unknown. This caused great uncertainty regarding the voltage loss over the current limiting resistances, and actual voltage applied to the cable objects.

Two sets of measurements were performed. The first with nothing connected to the source and the second with the arm switch connected to the circuit. The monitor voltage was measured in both cases, and when connected, also the voltage over $R = 472.6 \text{ k}\Omega$, see table 3.

Considering the effect of the switch, there was a significant change in current when applying more than 40 kV. Also when increasing the applied voltage, the difference between currents increased. The currents were calculated using equation 18 plotted using matlab, see figure 22.

In order to determine the voltage loss over the current-limiting resistance, the difference between the currents in figure 22 was multiplied with the resistance of $2.005 \text{ G}\Omega$. In addition, the voltage over R_2 was measured by the multimeter was used to find a comparable voltage loss, applying the relation:

Table 3: Monitor voltages without any equipment, and with arm switch in circuit.

<i>Applied voltage</i>	<i>U_m (nothing connected) [V]</i>	<i>U_m (breaker connected) [V]</i>	<i>U_r [V]</i>
0	0.015	0.014	0
20	0.044	0.045	0.044
40	0.083	0.091	0.447
60	0.113	0.183	1.28
80	0.186	0.263	2.29
100	0.231	0.352	3.78
120	0.273	0.454	5.9

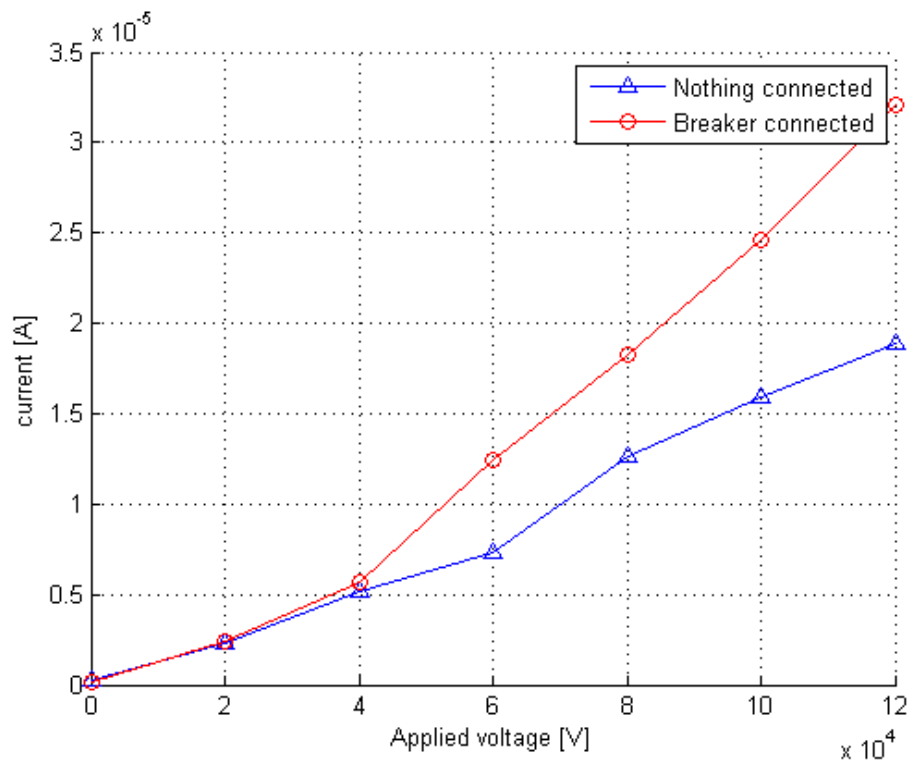


Figure 22: Currents with and without armbreaker in circuit.

$$U_{loss} = I_{circuit} \cdot 2.005 \cdot 10^9 \Omega = \frac{U_r}{472.6 \cdot 10^3 \Omega} \cdot 2.005 \cdot 10^9 \Omega \quad (19)$$

The voltage loss indicated by these two measurements was plottet with matlab, see figure 23.

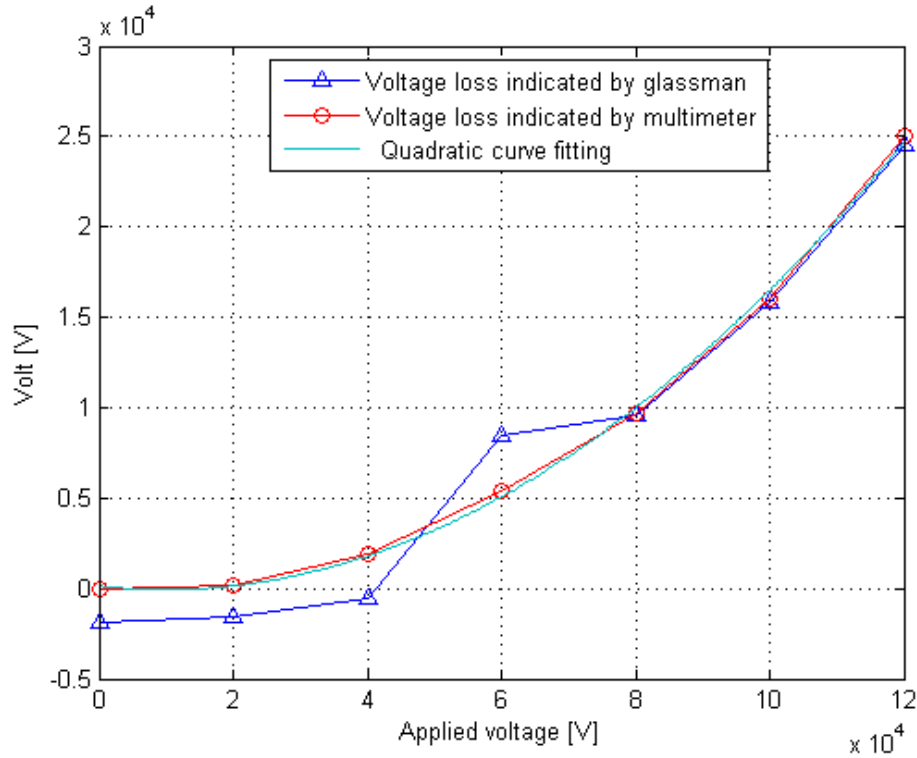


Figure 23: Calculated voltage loss with armbreaker in circuit.

Using the arm switch in the circuit, the voltage loss was quite significant. When applying a voltage of 50 kV the voltage loss was about 3 kV and when applying 100 kV, the voltage loss was about 16 kV. A relation between the applied voltage and the voltage loss was found, see equation 20.

$$U_{loss}(U_0[V]) = 2.04 \cdot 10^{-6} \cdot U_0^2 - 0.04 \cdot U_0 + 133[V] \quad (20)$$

3.3 Sphere switch

Due to the uncertainty of the arm switch, a more reliable alternative was needed. With basis in the IEEE publication "Standard Techniques for High-

Voltage Testing” a switch based on a sphere gap was created. The sphere gap used air as insulation material, and a more homogenous field distribution was provided than for the arm switch.

As a mechanism of applying the rapid voltage surges, a striker with a small tip radius was extended from the lower sphere into the gap. The electric field at the tip of the striker became so enhanced that the air broke down and an arc formed between the upper sphere and the striker tip.

As the impedance in figure 1 originally was connected between the lower sphere and ground, a voltage was set up over this as the grounding were performed. It was found that this voltage travelled back through the wires and discharged in the surge arresters, rendering the effect of the impedance useless. This was solved with placing the impedance between the HV-part of the switch and the cable object.

Additionally, on one occasion unexpected discharges occurred at a sphere gap with sufficient distance and without the striker extended. This was later found to be caused by a strand of hair that was situated on top of the lower sphere.

The IEEE publication supplied known withstand values for different setups of sphere diameter and sphere separation. And the measured withstand voltages of the sphere gap switch deviated no more than 3.58 % from the table values in [6], see table 4.

Table 4: Measured Gap distance and withstand voltage

<i>Arch gap [cm]</i>	<i>Withstand voltage [kV]</i>
3.77	110
5.02	140
7.35	190

$$D_1 = \frac{110 - 106.02}{106.02} \cdot 100 = 3.58\% \quad (21)$$

$$D_2 = \frac{140 - 137.48}{137.48} \cdot 100 = 1.83\% \quad (22)$$

$$D_3 = \frac{190 - 191.70}{191.70} \cdot 100 = -0.89\% \quad (23)$$

In order to visualize, the measured withstand values was plotted and compared to the table values using matlab, see 24.

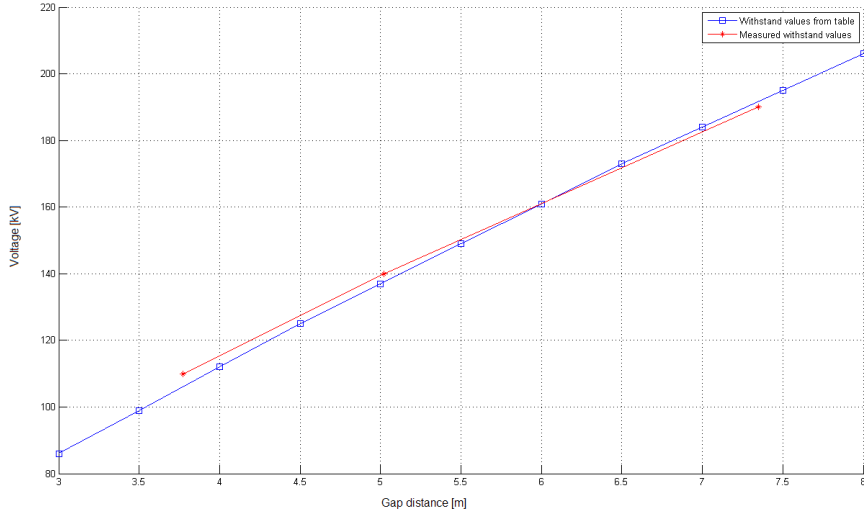


Figure 24: Measured withstand values and table values

The striker mounted in the lower sphere needed a more elaborate control system than provided by the relay and labview program. Hence a control circuit was created and tested.

Having designed the control circuit, the circuit was created and tested for faults with a simple voltmeter. When connected to the grid, the circuit worked properly and the needle stroke as intended. The input voltage was measured to 224.6 V. On the secondary side, the voltage was measured to 129.9 V. This gives the transformer a more accurate ratio of 1.73:1. The rectified dc voltage was also measured.

Table 5: Measured voltages from control circuit

<i>Point of measurement</i>	<i>Measured voltage [V]</i>
input voltage	224.6 VAC
transformed voltage	129.9 VAC
rectified voltage	177.1 VDC

The leakage currents of the sphere gap switch was measured using both the monitor voltage and the voltage that appeared over a resistance of 472.6 k Ω , see tables 20 - 22. The actual current measured through the sphere gap was found to be insignificant compared to the output current indicated by the glassman source. This is illustrated in figure 25 where the graphs are at the bottom are the currents measured by the multimeter.

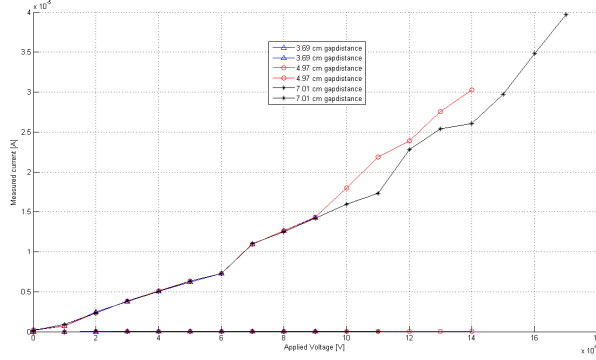


Figure 25: Breakdown channel in cable insulation

In table 21 and table 22 the voltage over the resistance R2 varied so much that the value was unable to be read. This occurred when about 110 kV and more was applied. There was also audible corona at these voltages. The largest voltage measured over the resistance was 0.003 V when applying 100 kV over a sphere gap of 4.97 cm. This indicated that a current of

$$I = \frac{0.003V}{472.6 \cdot 10^3 \Omega} = 6.35 \cdot 10^{-9} A \quad (24)$$

was flowing through the gap.

Assuming that the same current flows through the current-limiting resistances, the voltage loss would be:

$$U_{loss} = 6.35 \cdot 10^{-9} A \cdot 2.005 \cdot 10^9 \Omega = 12.73V \quad (25)$$

This value was considerably less than the voltage loss of 16 kV that occurred when applying 100 kV to the arm switch.

The values read from the multimeter were very small and in order to get comparative data the sphere gap was short-circuited and measurements performed. Using the short-circuit measurements in table 23, the indicated currents were compared to the calculated currents, see table 6.

In table 7 the deviation of the measured currents from the calculated current is shown, after applying equation 26.

$$\text{deviation [\%]} = \left| \frac{I_{calculated} - I_{measured}}{I_{calculated}} \right| \cdot 100 \quad (26)$$

3 RESULTS 3.4 Closer examination of the undetermined leaked current

Table 6: Voltages measured with shortcircuited gap and the currents they indicate

<i>calculated current</i> [μA]	<i>current through R2</i> [μA]	<i>current indicated by source</i> [μA]
0	0.00317	0.29
9.97	10.14	7.35
19.95	19.85	19.79
29.92	29.94	30.38
34.90	34.27	34.87

Table 7: Deviation of measured currents from calculated current

<i>Calculated current</i> [μA]	<i>Deviation R2</i>	<i>Deviation Glassman source</i>
0	-	-
9.97	1.71 %	24.37 %
19.95	0.50 %	0.80 %
29.92	0.03 %	1.50 %
34.90	1.78 %	0.09 %

As the sphere gap was found to have insignificant leakage currents, testing of a cable object was performed. The program detected a failure after 70 groundings. After slicing the cable object with a microtome, it was found that the distance from the needle tip to the inner semiconductor was about 3 mm, see figure 26

For this length, fronttime and voltage, the expected number of groundings was in the area of 60-100 groundings.

3.4 Closer examination of the undetermined leaked current

Undeterminable leakage currents was indicated by the voltage source. As no equipment was connected to the source, the monitor voltage indicated an output of as much as 15.88 μA when applying 100 kV, 25.45 μA when applying 160 kV and as much as 31.54 μA when applying the maximum voltage of 200 kV, see figure 27. If this current was flowing through the circuit, it would cause great voltage losses and a reduced voltage applied to the cable objects.

Even though a current was indicated, this was not the same as measured in the actual circuit. The sphere gap was found to have insignificant leakage

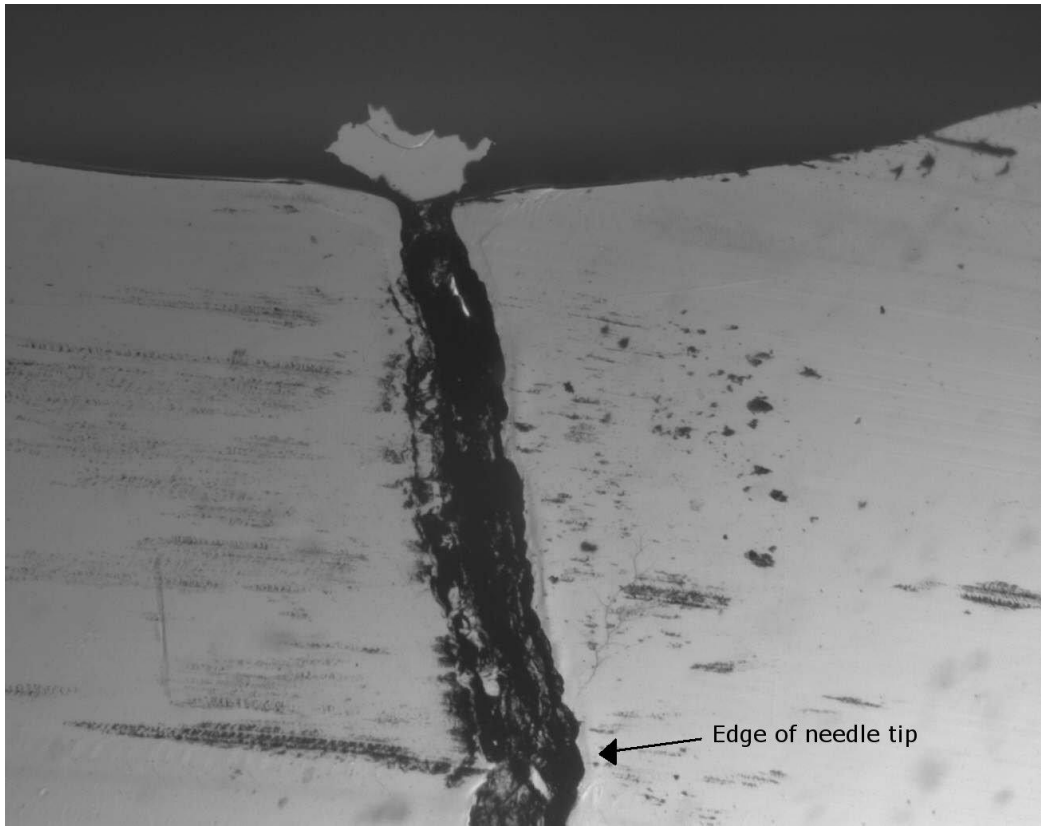


Figure 26: Breakdown channel in cable insulation

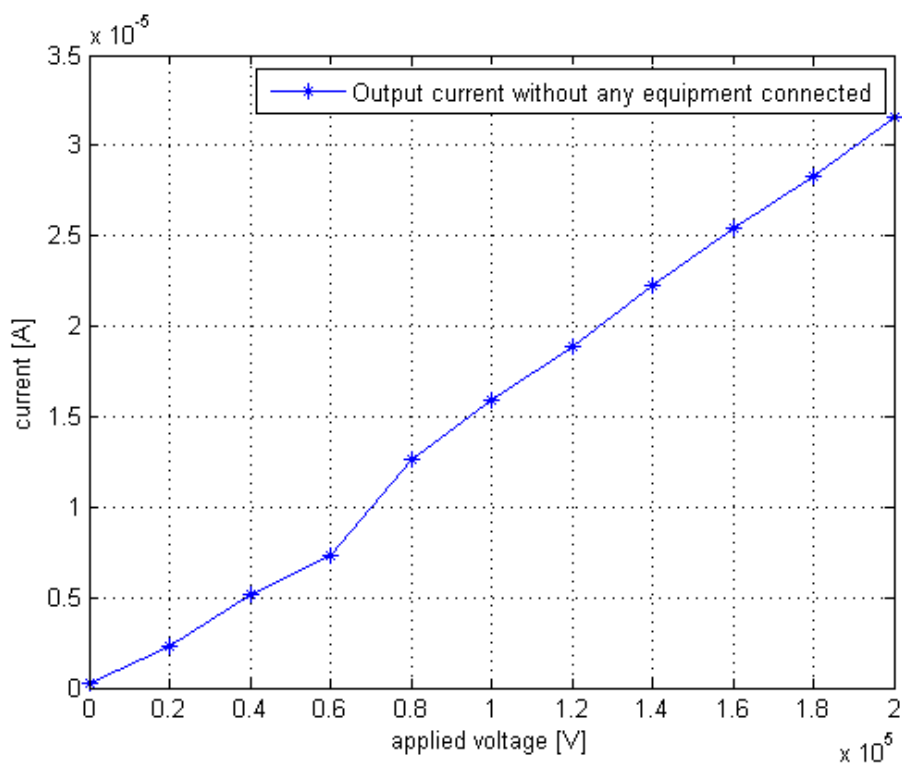


Figure 27: Measured current with no equipment connected.

currents when subjected to voltage. The armswitch had significant leakage currents that corresponded only to the increase in monitor voltage, but not the total current indicated by the monitor voltage.

After a more thorough inspection of the circuit schematics of the voltage source, a voltage-divider was found to be present inside the source, as in figure 28. The purpose of this voltage divider was to derive a feedback signal for monitoring the real output voltage.

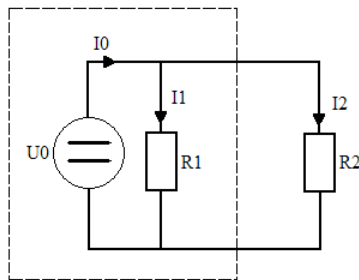


Figure 28: Inner resistance of source

The actual value of the resistance in the divider was not described in the manual. However, the manual stated that a signal varying from 0 V to 10 V is in direct proportion to the output current.

Assuming that a monitor voltage of 0 V indicates no current, and a monitor voltage of 10 V indicates the rated current of 1 mA as in figure 29, the assumed relation between monitor voltage and output current was described as in equation 27.

$$I = \frac{U_m}{10} \cdot 0.001 \tag{27}$$

In order to determine the value of R_1 figure 28, the values in table 23 was used, except the measurement for zero applied voltage. These measurements were done with the known R_2 equal to $2.0054726 \text{ G}\Omega$ and the control measurement using the multimeter. Knowing the current I_2 that flows through R_2 , the current I_1 can be determined subtracting I_2 from the assumed total current, $I_1 = I_0 - I_2$. And further the resistance of the voltage divider can be found using Ohms law on I_1 and the applied voltage, see table 8

3 RESULTS.4 Closer examination of the undetermined leaked current

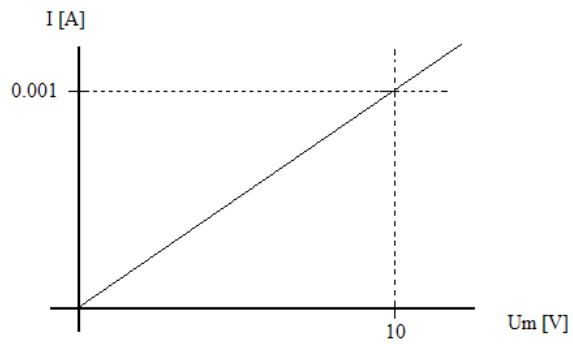


Figure 29: Relation between monitor voltage and output current

Table 8: Calculated current and resistance in voltage divider

$U0$ [kV]	$I0$ [microampere]	$I2$ [microampere]	$I1$ [microampere]	R [GOhm]
20	11.6	9.97	1.63	12.27
40	28.5	19.95	8.55	4.68
60	43.1	29.92	13.18	4.55
70	49.3	34.90	14.4	4.86

3.4 Closer examination of the undetermined leaked current RESULTS

When disregarding the first calculated resistance, the average resistance of R1 was calculated to be

$$R_{average} = \frac{(4.68 + 4.55 + 4.86) \cdot 10^9}{3} \Omega = 4.6966 \cdot 10^9 \Omega \approx 4.70 \cdot 10^9 \Omega \quad (28)$$

This value of R1 was found using measurements when equipment was connected to the source. These values were further tested using the values from table 3 when no equipment was connected, rendering R2 as an open circuit. It was then assumed that all the current indicated by the source was flowing through the calculated resistance R1. In table 9, the assumed current found using equation 27, I1a, was compared to the current calculated using Ohm's law with the applied voltage and resistance found in 28, I1b. The deviation of I1b from I1a was found using:

$$\text{deviation [\%]} = \left| \frac{I1a - I1b}{I1a} \right| \cdot 100 \quad (29)$$

Table 9: Calculated currents through R1

$U0$ [kV]	Um [V]	$I1a$ [microampere]	$I1b$ [microampere]	Deviation[%]
20	0.044	4.4	4.26	3.18
40	0.083	8.3	8.51	2.53
60	0.113	11.3	12.77	13.00
80	0.186	18.6	17.02	8.49
100	0.231	23.1	21.28	7.88
120	0.273	27.3	25.53	6.48

4 Discussion

The program was not set to handle the errors messages that may be generated from the instrument. This means, that if unexpected events and error-messages occur, the program will not be able to handle them.

Even though the output current and the current flowing in the circuit was found to be different, the relation used to indicate failure will still be valid as the voltage applied to the circuit will be the same.

The voltages in figure 22 are quite equal for low voltages, hence the uncertainty of the difference between them is greater than for that measured by the multimeter. Therefore, the current measured by the multimeter was used by the regression tool in matlab, to find a quadratic relation between the applied voltage and the voltage loss, see equation 20.

Leakage currents was measured and found to be insignificant in the sphere gap. Although the spheres do not have smooth surfaces as required from [6], corona discharge may occur for higher voltages. Additionally

The largest measured leakage current was calculated to cause a voltage loss of 12.73 V when applying 100 kV. A voltage loss considerably smaller than the 16 kV of voltage loss caused by the armbreaker.

When the sphere switch was found not to cause any voltage loss, a breakdown test was performed on a cable object. A needle was inserted leaving 3 mm of healthy insulation between the needle tip and the innermost semiconductor. The expected number of voltage surges needed to cause a breakdown was between 60 and 100. The program detected a failure after 70 surges, which was a bit lower than expected.

The low number of surges that was needed is believed to be caused by the different setup of the circuit when connecting the sphere switch. The upper sphere is connected to the front-time resistance with a copper wire of broader cross-section and lesser transition resistance than previously used. This is believed to provide a more rapid discharge in the insulation around the inserted needle and faster initiation of electrical treeing. This may also mean that reproducing old results may be difficult as the setup of the circuit has been changed.

The circuit was designed from concept and only tested with series of no more than 226 groundings. Hence, it should be reconstructed in case of extended use in order to remove eventual flaws and secure better long-term stability.

The sphere gap was also found to be sensitive to pollution, e.g. dust and small conductive particles that may change the electric field. For instance, a strand of hair was found to cause breakdown in the gap when applying 95 kV to a gap distance of 35 mm. This raises the need for clean electrodes and surroundings when voltage surges are to be applied.

5 Conclusion

A program was designed and created using Labview as a control system for instruments using the GPIB standard interface. The program created was proven to correctly indicate a failure in a cable object.

An arm switch was constructed in order to improve the reliability of an already existing construction. The constructed arm switch was found to have a leakage current proportional to the square of the applied voltage, see equation 20. Due to this voltage loss, the armbreaker was not suitable for use in the automation of the rapid voltages surges subjected to cable objects.

A sphere gap switch was constructed, based on international standards for measuring high voltage. The constructed sphere switch was found to have insignificant leakage currents and a test of a cable object was performed and found to be reasonably coherent with previous experience.

Throughout the work, undetermined output currents was indicated from the source. As no apparent paths was found, the source was closely examined and an internal voltage divider was found present in the Glassman high voltage source. The current was found to flow internally in the source and not in the test circuit, causing voltage losses.

6 List of devices

The following devices were used in the project:

Table 10: List of devices

<i>Device number</i>	<i>Device</i>
B02- 0313	Mascot 0-30V voltage source
B2-321	Glassman high voltage source
G04-0026	Yokogawa Oscilloscope
G05-0101	HP Agilent Datalogger
S03-0356	Fluke Multimeter
B01-0491	Skilletrafo
SEFAS I04-0402	Voltage divider
H01-0094	Megger
K3-083	100 pF capacitor
K3-68	100 pF capacitor

References

- [1] Agilent Technologies. *Agilent 34970A Data Acquisition/Switch Unit Users Guide*, third edition, 1999.
- [2] Dr B.R. Andersen, editor. *HVDC transmission - Opportunities and challenges*. Andersen Power Electronic Solutions Ltd, UK, 2006.
- [3] J.Kuffel E. Kuffel, W.S.Zaengl. *High Voltage Engineering: Fundamentals*. Newnes, second edition, 2000.
- [4] Erling Iland and Mildrid Selsjord. *DC Treeing and Breakdown of XLPE Insulation during Rapid Voltage Grounding*. Technical report, Norwegian University of Science and Technology, 2005.
- [5] Glassman high voltage inc. *Instruction manual, PG series*, third edition.
- [6] The Institute of Electrical and Electronics Engineers. *IEEE Standard Techniques for High-Voltage Testing*, 1995.
- [7] Mildrid Selsjord and Erling Ildstad. *Electrical Treeing Caused by Rapid DC-Voltage Grounding of XLPE Cable Insulation*. Technical report, SINTEF Energy Research, Sem Sælandsvei 11, 7465 Trondheim, 2005.
- [8] 'National Instruments'. *'LabVIEW. GPIB and Serial Port VI reference manual'*, august 1993.
- [9] P. Osmokrovic, N. Arsic, and N. Kartalovic. *Triggered Vacuum and Gas Spark Gaps*. IEEE Transactions on Power Delivery, 11, 1996.
- [10] P. OsmoKrovic, N. Arsic, Z. Lazarevic, and D. Kusic. *Numerical and Experimental Design of Three-electrode Spark Gap*. IEEE Transactions on Power Delivery, 9, 1994.
- [11] Thomas Karlsen. *Testing of HVDC cables using rapid voltage surges*. Project thesis, Norwegian University of Technology and Science, 2006.

A Monitor voltage and output current

Table 11: Measured monitor voltage and calculated current.

U [kV]	U_m [V]	Calculated current [microA]
0	0.015	0
10	0.071	4.99
20	0.144	9.97
30	0.218	14.96
40	0.287	19.95
50	0.357	24.93
60	0.427	29.92
70	0.494	34.90
80	0.558	39.89
90	0.625	44.88

B Maximum E-field at electrode surface

Table 12: distance = 0.075 m

Electrode radius [m]	Maximum electric field [MV/m]
0.01	6.5
0.02	4.5
0.03	3.8
0.04	3.5
0.05	3.4

Table 13: distance = 0.1 m

Electrode radius [m]	Maximum electric field [MV/m]
0.01	5.7
0.02	3.9
0.03	3.3
0.04	2.9
0.05	2.7

B MAXIMUM E-FIELD AT ELECTRODE SURFACE

Table 14: distance = 0.125 m

<i>Electrode radius [m]</i>	<i>Maximum electric field [MV/m]</i>
0.01	5.1
0.02	3.45
0.03	2.4
0.04	2.5
0.05	2.3

Table 15: distance = 0.15 m

<i>Electrode radius [m]</i>	<i>Maximum electric field [MV/m]</i>
0.01	5.0
0.02	3.2
0.03	2.6
0.04	2.3
0.05	2.1

Table 16: distance = 0.175 m

<i>Electrode radius [m]</i>	<i>Maximum electric field [MV/m]</i>
0.01	4.6
0.02	3.6
0.03	2.3
0.04	2.0
0.05	1.9

Table 17: distance = 0.2 m

<i>Electrode radius [m]</i>	<i>Maximum electric field [MV/m]</i>
0.01	4.4
0.02	2.6
0.03	2.2
0.04	1.9
0.05	1.7

Table 18: distance = 0.225 m

<i>Electrode radius [m]</i>	<i>Maximum electric field [MV/m]</i>
0.01	4.1
0.02	2.6
0.03	2.1
0.04	1.8
0.05	1.6

C VOLTAGES MEASURED WITH SPHERE SWITCH

Table 19: distance = 0.25 m

<i>Electrode radius [m]</i>	<i>Maximum electric field [MV/m]</i>
0.01	4.1
0.02	2.5
0.03	1.95
0.04	1.7
0.05	1.5

C Voltages measured with sphere switch

Table 20: Voltages measured with 3.69 cm gap distance

<i>U [kV]</i>	<i>Um [V]</i>	<i>UR2 [V]</i>
0	0.014	0
10	0.022	0
20	0.046	0
30	0.064	0.001
40	0.082	0.001
50	0.098	0.001
60	0.113	0.0015
70	0.163	0.002
80	0.186	0.002
90	0.209	0.002

C VOLTAGES MEASURED WITH SPHERE SWITCH

Table 21: Voltages measured with 4.97 cm gap distance

U [kV]	U_m [V]	UR_2 [V]
0	0.015	0
10	0.022	0
20	0.044	0.001
30	0.065	0.001
40	0.083	0.001
50	0.099	0.001
60	0.113	0.0015
70	0.163	0.002
80	0.186	0.002
90	0.210	0.003
100	0.260	0.003
110	0.314	–
120	0.342	–
130	0.392	–
140	0.430	–

Table 22: Voltages measured with 7.10 cm gap distance

U [kV]	U_m [V]	UR_2 [V]
0	0.014	0
10	0.025	0
20	0.044	0.001
30	0.065	0.001
40	0.082	0.001
50	0.099	0.001
60	0.113	0.001
70	0.164	0.002
80	0.185	0.002
90	0.208	0.002
100	0.232	0.002
110	0.251	0.0025
120	0.327	–
130	0.362	–
140	0.372	–
150	0.422	–
160	0.492	–
170	0.560	–

Table 23: Voltages measured with shortcircuited gap.

U [kV]	U_m [V]	$UR2$ [V]
0	0.016	0.0015
20	0.116	4.79
40	0.285	9.38
60	0.431	14.15
70	0.493	16.20